Jet Stream Analysis and Forecast Errors Using GADS Aircraft Observations in the DAO, ECMWF, and NCEP Models

Carla Cardinali (ECMWF), Leonid Rukhovets (SAIC and DAO/ NASA Goddard), and Joel Tenenbaum (SUNY at Purchase)

Summary

We have utilized an extensive set of independent British Airways flight data recording wind vector and temperatureobservations (the Global Aircraft Data Set [GADS] archive) in three ways:
(a) as an independent check of operational analyses;
(b) as an analysis observing system experiment (OSE) as if the GADS observations were available in real time; and
(c) as the corresponding forecast simulation experiment applicable to future operational forecasts.
Using a 31 day sample (0000 UTC 20 December 2000 through 0000 UTC 20 January 2000) from Winter 2000, we conclude that over the data-dense continental U. S. analyzed jet streaks are too weak by -2% to -5%. Over nearby data-sparse regions of Canada, analyzed jet streaks are too weak by -5% to -9%. The second range provides a limit on the accuracy of current jet streak analyses over the portions of the ~85% of the earth's surface that are poorly covered by non-satellite observations. The -5% to -9% range is relevant for the pre-third generation satellite (AIRS, IASI, GIFTS) era.

The manuscript will be submitted to *Mon. Wea. Rev.*

Jet Stream Analysis and Forecast Errors Using GADS Aircraft Observations in the DAO, ECMWF, and NCEP Models

Carla Cardinali

European Centre for Medium Range Weather Forecasts, Reading, England

Leonid Rukhovets

SAIC and NASA Goddard Data Assimilation Office, Greenbelt, Maryland

Joel Tenenbaum[1]

State University of New York Purchase, New York

[1] *Corresponding author address*: Joel Tenenbaum, Division of Natural Sciences, State University of New York, Purchase, NY 10577. E-mail: joel@zephyr.ns.purchase.edu.

ABSTRACT

We compare peak analyzed jet stream wind speeds with independent aircraft observations over Canada and the continental U. S. The results permit study of the accuracy of jet streak strength for the data-sparse 85% of the earth's surface versus the data-dense 15%. The observations come from the Global Aircraft Data Set (GADS) experiment which since 1996 has collected flight data recorder information from every flight of 56 British Airways 747-400 aircraft. The study is timely because automated aircraft observations are reaching their near-asymptotic limits (there are not many uncovered commercial aircraft routes left) and we are about to enter a new, third generation, satellite sounding instrument era. Future reanalyses will mix time periods from both eras. This study allows an estimate of the pre-third generation accuracy.

Our results are that major current generation assimilation models have peak wind speed errors of -5% to -9% over data-sparse Canada compared with -2% to -5% over the data-dense continental U. S. When these additional aircraft observations are incorporated as a simulated part of the normal observational input data stream, we show a small but statistically significant improvement in an ensemble of ECMWF forecasts.

1. Introduction

In this study we address two related questions: how accurately are strong jet streams depicted in analyses and what effect can additional aircraft data have on forecasts? Inaccurate jet streams in analyses and forecasts have a direct effect on the accuracy of energy and moisture transports and, for forecasts, in baroclinic developments. We use automated aircraft observations from the Global Aircraft Data Set (GADS) experiment. The GADS experiment collects information from flight data recorders of British Airways 747-400 aircraft unconstrained by the cost limitations of real-time transmissions (e.g. AMDAR[2]; ACARS[3], Benjamin et al. 1999). The GADS observations are independent of the transmissions used by operational centers. Our audience is twofold: modelers working in weather and climate and the aviation community trying to determine the value of transmitting additional aircraft observations in real time. The latter group seeks an answer to the question: do additional observations transmitted in real time provide enough benefits to justify their additional cost?

Several factors make this study relevant now. The efforts of the WMO AMDAR panel have produced a qualitative and, to an

---

[2] Aircraft Meteorological DAta Reporting; see http://www.metoffice.com/research/interproj/amdar/index.html

[3] Aircraft Communications Addressing and Reporting System

extent, asymptotic, increase in some sparse-area aircraft data densities. With the possible exception of Russia and China, there are not too many uncovered long-haul commercial aviation routes left. Separately, the U. S. and EUMETSAT will soon launch the next (third) generation of satellite sounders (AIRS, IASI, Cheury et al. 1993; GIFTS) which should improve the global determination of winds. For future reanalyses, we need to know what biases existed prior to the availability of these third generation satellite instruments.

In contrast to our previous studies of this type (Tenenbaum 1991, 1996; Rukhovets et al. 1998; Rickard et al. 2001) which dealt primarily with Asia, for this study we stress Canada and the contiguous U. S. The U. S. is extremely well covered by ACARS observations (Benjamin et al. 1999). In comparison, just prior to the recent increase in automated aircraft reports over Canada, that area, though adjacent to the dense U.S. coverage, presented cases in several global models with large errors relatively near the U. S. border.

Atmospheric variables in current multivariate assimilation systems are determined from a number of sources including directly from radiosondes and aircraft observations and indirectly from the second generation of satellite sounders. Comparisons with independent aircraft observations over Canada can quantify errors in analyzed jet streak maxima for regions

lacking significant conventional observations. They allow insight into the large geographical areas where additional aircraft data will not be available due to a lack of any routes or, at least for the next decade, routes flown by technically sophisticated long-haul carriers. For future reanalyses, our results provide an indication of the magnitude of jet stream errors in regions where we will never be able to get accurate aircraft observations and provide a technique for calibrating winds from analyses incorporating radiances from the next generation of satellite instruments. Specifically, we use the result (Rukhovets et al. 1998) that dense (~ every 25 km) aircraft wind observations determine atmospheric wind speeds *independent of any specific assimilation system.*

2. Aircraft Observation Techniques

Wide-bodied aircraft measure wind and temperature as a routine part of their navigation and operating procedures. These measurements are comparable to radiosonde accuracies for vector wind error (±1-2 m s^{-1}; WMO 1996) and only slightly worse for temperatures (±0.85 °C; WMO 1996). A collocation study using ACARS observations (Benjamin et al. 1999) obtains standard deviations of 1.1 m s^{-1} for a single horizontal component of wind and 0.5 °K for the temperature above the boundary layer.

Once an aircraft observation has been made, two types of procedures are then used to transfer the observation to the meteorological Global Telecommunications System (GTS): voice (AIREP) and automated satellite or VHF radio transmissions (AMDAR and ACARS). Because of garbles and transcription errors, AIREPs have an effective vector wind error of 2-4 m s^{-1} while automated reports retain the underlying accuracy of the measurements.

Cost considerations limit automated transmission rates. But for historical reasons, certain carriers record winds speed and temperatures onto flight data recorders much more frequently than the AMDAR specification of 7.5 min intervals. British Airways (BA) records at 4 sec intervals. The GADS experiment (Rukhovets et al. 1998, Rickard et al. 2001) has made use of this higher recording frequency and sampled the BA winds and temperatures from every flight of each BA 747-400 aircraft since 1996. The sampling is done at 128 sec (1996-2001) and 32 sec (2002-) intervals. Earlier versions (Tenenbaum 1991) of this experiment also collected data from Japan Airlines and Lufthansa.

Long-haul aircraft routes are chosen so that, where possible, the planes fly close to jet cores (eastbound) and avoid them (westbound) for many of the trans-Atlantic and trans-Pacific flights. Other routes cross the jets approximately perpendicularly (South Asia, polar routes from Europe to the west coast of North America). The maximum winds encountered by

aircraft provide a clear measure of the accuracy of analyzed and forecast jets. Via the thermal wind relationship, these wind maxima also indicate the accuracy of thermal gradients associated with baroclinicity and climatological transports.

3. Detailed Procedures

To check the performance of operational analyses, we use the two synoptic times at 0000 and 1200 UTC and interpolate the analyses to the time of the jet streak crossing. Our comparisons are with high resolution global assimilation systems from two operational forecast centers (European Centre for Medium Range Weather Forecasts, ECMWF; U. S. National Centers for Environmental Prediction, NCEP) and one operational analysis center (the NASA Goddard Space Flight Center Data Assimilation Office, DAO). A separate comparison of GADS observations with the global United Kingdom Meteorological Office (UKMO) model has recently been published (Rickard et al. 2001). Two other models and assimilation systems are relevant to this area. The Canadian Meteorological Centre global and regional models (GEM; Cote et al. 1997; Chouinard et al. 1999) use a 3-dimensional variational (3DVAR) approach plus a uniform 0.9° grid for the global version and 0.36° grid for the regional model over Canada and the U. S. The NOAA Forecast Systems Laboratory (FSL) Rapid Update Cycle (RUC) model makes maximum use of the ACARS observations over the

continental U. S. (Benjamin et al. 1999). It relaxes to the performance of the NCEP regional Eta model north of the Canadian border. Comparisons with the two regional models could not necessarily be extrapolated to a global domain.

While some centers archive data at 0600 and 1800 UTC, use of the 0000 and 1200 UTC synoptic times allows us to maintain comparability among all centers. Similarly, we concentrate on the large number of flights at levels close to 250 hPa (33 000 ft and 35 000 ft; near the optimal engine performance level for modern three- and four-engine subsonic jet aircraft) to minimize vertical interpolation errors.

We compare the maximum wind speed encountered by the aircraft with the maximum wind speed of the analysis or forecast. As noted above, most long-haul aircraft routes can be divided into two categories in relation to their jet crossings: perpendicular and parallel. Because of the sharp gradients near jet streams, small changes in the exact position in space and time of a jet streak could cause the "point" value[4] of the analyzed and forecast wind speed to seem unreasonably weak. Specifically, current global model grid spacings of approximately 60-80 km are comparable to the transverse scale of strong jet streaks.

---

[4] i.e., the wind speed from the analysis or forecast at the exact latitude and longitude of the jet streak maximum observed by the aircraft.

To compensate for this problem, we compare the peak wind speed encountered by the aircraft with the peak wind along or adjacent to the aircraft track within a distance related to jet streak movement or model resolution. (In subsequent discussions, these two approaches are referred to as the "point" and "path" values.) For analyses and forecasts with flight paths *perpendicular* to the jet stream we define the "path" value as the maximum wind speed *along* the aircraft flight path interpolated between the bounding synoptic times. This situation is illustrated in Figs. 1a and 1b where the jet streak axis at 1200 UTC 26 December 1999 is just southwest of where the aircraft found the peak wind speed (i.e., the "point" value) and the jet streak axis at 0000 UTC 27 December 1999 is northeast of the point value location. For this London - San Francisco route path maxima of 71 m s^{-1} and 92 m s^{-1} from the two synoptic map times were time-interpolated to 87.0 m s^{-1} valid at the observed maximum crossing time of 2109 UTC 26 December 1999.

For flight paths parallel to the jet stream, we allow displacements of up to 160 km *perpendicular to* the aircraft flight path and jet axis. The value 160 km represents 2) for the current (2001) NCEP analysis resolution which is the median of the three centers covered. A typical case with a displacement to the jet streak axis of about 50 km is shown in Figs. 2a and b which illustrate the uncertainties when the aircraft route is parallel to the jet streak. Here path maxima on the axes of 91 m

s^{-1} and 93 m s^{-1} were time interpolated to a value of 92.4 m s^{-1}.

Our data was taken during two observational time periods

Table 1: Observation dates for the analysis (Winter 2000) and forecast (both winters) comparisons.

Label	Start	End
Winter 1999	0000 UTC 01 January 1999	0000 UTC 24 January 1999
Winter 2000	0000 UTC 20 December 1999	0000 UTC 20 January 2000

It includes all strong (> 50 m s^{-1}) jet cases occurring during the indicated periods. As noted above, vertical interpolation was avoided by using flights near the standard 250 hPa level. Horizontal interpolation perpendicular and parallel to the path was performed using high resolution maps generated by the centers themselves using their full resolution archived data (e.g, 0.5° x 0.5° for ECMWF).

4. Analysis Results

a. Canada versus U. S.

The global distribution of automated aircraft observations is very non-uniform as illustrated in Fig. 3a for 0000 UTC 17 March 2001. Recent observation counts are dominated by the ACARS

reports over the continental U. S. and the dense North Atlantic track region. But as can be seen by examining the secular changes in an enlarged view centered on the U. S. - Canadian border region (Fig. 3b for 0000 UTC 17 March 1999, typical for the period covered by this study, and 3c for 0000 UTC 17 March 2001, the same as in Fig. 3a) as a result of efforts of the WMO AMDAR panel this situation has changed. The two time periods listed in section 3 precede the recent increase in ACARS and AMDAR observations over Canada illustrated in Figs. 3a and 3c.

This sharp density contrast at the U. S. - Canadian border for 1999 and 2000 allows us to examine a key question concerning the accuracy of jet streams in analyses: what is the absolute error in data-sparse and data-dense regions? Such errors will affect reanalyses (Kanamitsu et al. 1999; Uppala et al. 1999) as the next (third) generation of satellite instruments begins to be incorporated into major assimilation systems and the reanalysis periods effectively include time segments with and without third generation satellite sounder observations.

Our primary analysis result is illustrated in Table 2 for Winter 2000. Winter 1999 did not have enough days with strong jets over Canada to permit a meaningful comparison.

Table 2. Percent error in peak wind speed (analysis value minus aircraft value divided by aircraft value) for 0000 UTC 20 December 1999 through 0000 UTC 20 January 2000 (referred to as Winter 2000) of analyzed wind speed for the three centers used stratified by region and center.

	cases	mean wind speed ($m\ s^{-1}$)	DAO (%)	ECMWF (%)	NCEP (%)
Canada	15	74.7	-8.9	-5.0	-8.0
U. S.	20	73.1	-4.6	-2.1	-2.1
difference			-4.3	-3.0	-6.1

Three conclusions follow from the results in Table 2: First, away from the continental U. S. with its dense ACARS coverage, all three global models still have average peak wind speed errors of at least 5%. Second, current generation assimilation systems can determine the peak strength of their jet streams in data sparse areas to an average accuracy of -5% to -9%. Third, the NASA DAO analyses are comparable to the operational forecast centers. The corresponding numbers for the data-sparse southwest Asian region for a previous generation of assimilation systems were -11% to -17% (Tenenbaum 1991).

It is important to note limitations and possible problems between the Canadian and U. S. values. First, the winter time period contains the strongest portion of the annual cycle of

winds. As illustrated in Rickard et al. (2001, Fig. 6), errors in wind speed analyses do increase with the strength of the jet stream. Second, there could be a directional dependence. There are more northwesterly jets in the Canadian sample than in the U. S. sample. Third, the jets studied are near 250 hPa and there could be a height dependence. There is some change of the average height of the polar jet over the latitude range between Canada and the U. S. Fourth, information from the data-dense continental U. S. could be propagating upstream explicitly (ECMWF 4-dimensional variational analysis) or implicitly (DAO and NCEP). Fifth, the BA aircraft observations are effectively point measurements (representative values over 4 sec or approximately 1 km) while the analysis values are averaged over one grid point (approximately 60 km for ECMWF). We have shown elsewhere (Rukhovets et al. 1998) that the averaging process changes error values by the order of 1%.

b. Changes in the analyses when GADS observations are included

To examine the effects of the additional GADS observations, we have rerun the assimilations with the GADS observations included in the input data stream. Because of computer time limitations on their primary computers, this approach was only feasible for DAO and ECMWF. In this section we examine the effects on the analyses and in the next section on the forecasts. The analysis and forecast performed by adding GADS

data are indicated as Winter 1999 and Winter 2000 for the periods shown in Table 1. The corresponding control experiments are denoted by Control.

Modern data assimilation systems at the major operational centers (Daley 1991, Parrish and Derber 1992, Courtier et al. 1993, Pfaendtner et al. 1994, McNally et al. 2000) combine incoming observations with a first guess (6-hour forecast) from a previous time step. Assimilation systems tend to smooth sharp gradients and, especially near strong jets, do not draw well to strong wind observations. In rapidly developing synoptic situations (e.g. the Christmas 1999 European storms; Saunders, 1999; Reale, private communication), there is an underlying tension. Too loose a cutoff on observations differing substantially from the first guess can introduce erroneous observations. Too tight a cutoff can miss baroclinic developments.

Fig. 4a shows the GADS observation superimposed on the ECMWF analysis for the difficult 1200 UTC 25 December 1999 case associated with the storms. Note the rejected AIREPS at approximately 46°N, 35°W. Fig. 4b shows the corresponding 1-dimensional wind speed plot for GADS observations, ECMWF Control analysis, and ECMWF GADS analysis. The ECMWF GADS analysis better depicts the trough between the two jet streaks but still cannot correctly depict the peaks.

Away from data-sparse regions, the GADS observations have a limited impact. One would expect very little effect from additional data over the continental U. S. and over the North Atlantic. As shown in Fig. 3, these areas are already quite well covered by aircraft observations. In terms of the focus of this paper on the U. S. - Canadian border contrast, there are still cases where there is a visible impact. Quantitatively these represent about 20% of the cases studied. In terms of commercial aviation operations, such cases do matter

A typical situation is shown in Fig. 5 for both ECMWF and DAO analyses. By comparing the control analyses (Figs. 5a and 5c) with the difference plots (Figs. 5b and 5d), we can see that the primary changes are associated with the gradients at the jet entry, exit, and sharp shear locations. This result is consistent with the previous ECMWF Christmas storm case (Fig. 4) and *does not* imply that the analyzed core wind speeds including GADS observations are now correct but simply that current analysis procedures cannot assimilate the full impact of these observations.

Clearly, the errors in these cases, while surprisingly close to (Figs. 5a and 5b) or over (Figs. 5c and 5d) a data-dense region, would not have a substantial effect on BA polar routes to the West Coast of North America. (They would affect

trans-Canadian routes more.) But in analogy with the discussions in Tenenbaum (1991, 1992) if jet cores are off by their current -5% to -9% values in other data-sparse regions, there are flights (South Asia, Africa, the Pacific) where there would be a significant operational impact.

5. Forecast Results

In the previous section the GADS observations were used as an independent check on the analyses or as a simulated part of the incoming observational data stream. We now examine the resulting forecasts for apparent differences on both a mean and case study basis. For the forecast impacts, we concentrate on the ECMWF results. That center has several advantages - higher resolution models, 4-dimensional variational analyses, a later cutoff time, and others - which have, in part, led to consistently better scores for the ECMWF forecasts, especially over their time period of primary concern (3-7 days). In the context of commercial aviation, from past experience, the improved resolution and later cutoff time indicate what will be possible at the operational centers a few years in the future.

In contrast to the data-dense U. S. and North Atlantic regions, both Russia and Canada have sparse enough data that the existing GADS observations are likely to have a visible impact.

For the Asian portion of Russia, there are relatively limited aircraft observations and growing problems with the functioning of the conventional radiosonde network (ECMWF Global Data Monitoring Report, private communication). Here any GADS observations represent a significant increment to observed data. For Canada we have more observations in the conventional radiosonde network. But the GADS aircraft are likely to have a larger impact when there are stronger jets.

We present in Fig. 6a and 6b the 300 hPa mean geopotential height contours for Winter 1999 and Winter 2000 periods. The Greenland cut off low is deeper into eastern Canada and the northeastern United States in Winter 2000 (Fig. 6b). This was manifested by the prevalence of a stronger northwesterly flow over western Canada during Winter 2000 compared with Winter 1999. Moreover, the well pronounced trough over South Europe in Winter 2000 (Fig. 6b) is replaced by a mean zonal flow in Winter 1999 (Fig 6a). In other words, the extra information provided by GADS data (see Fig. 7 below) can affect the flow that influenced the weather of United States and Europe by better determining the upstream jet streaks in Winter 2000 than Winter 1999.

The time average Eady index (Hoskins and Valdes 1990) is also shown in Figs. 6a and 6b, for the 700-850 hPa layer. This

quantity characterizes the regions of strong baroclinicity. A main region near Alaska in Winter 1999 is not present in Winter 2000, the instability over the west Atlantic is reduced in Winter 2000, and the index values in central Canada, Greenland, and North of South Arabia are well defined in Winter 2000 but not in Winter 1999. Comparisons with the daily GADS data coverage (Fig. 7) show that these data provide information on the unstable areas existent in Winter 2000 but not in Winter 1999. In particular, Fig. 7 depicts only the portion of GADS routes not covered by other aircraft used in the analysis experiments.

Our primary forecast results for Winter 2000 are illustrated in Fig. 8 where a 24 hour vector wind root mean square error (rmse) at 500 hPa is averaged over the European (Fig. 8a), North Atlantic (Fig. 8b), North American (Fig. 8c) and North Pacific (Fig. 8d) regions, respectively. All the forecasts are verified against their own analyses. The scatter plot shows that Winter 2000 is significantly (0.1% level for the Student's t-test) better than Control in all the regions (22 cases) whilst Winter 1999 indicates for the same forecast range (14 cases) a neutral impact (not shown). In the short range forecast (up to day 3), Winter 2000 performs better than Control and Winter 1999 shows no impact.

In Fig. 9a and 9b are shown the 500 hPa geopotential height

anomaly correlation for Winter 1999, Northern Hemisphere (Fig. 9a) and Southern Hemisphere (Fig. 9b), respectively. For the medium range forecast, Winter 1999 shows a slightly positive impact (from day 4) over the Northern Hemisphere and a slightly negative one over the Southern Hemisphere at day 5 (neutral afterwards). The forecasts have been verified against radiosonde observations (24 cases) but similar results are obtained for verification against the model's own analyses. The same forecast verification is shown, for Winter 2000, in Fig. 10. In the Northern Hemisphere (Fig. 10a) the slightly positive impact is consistent at all forecast ranges (becoming neutral at after day 6) whilst in the Southern Hemisphere it is positive only after day 5. The Winter 2000 positive impact on the short range forecast (Fig. 8) is kept in the medium range.

The different impacts of the GADS observations in the two winters, mainly in the short range forecasts, are probably due to the large scale flow differences in the two winter periods examined. In Winter 2000, the incremental GADS data distributions matched important baroclinic areas and, hence, have positively affected the analysis and the ensuing forecast.

6. Conclusions

We have utilized an extensive set of independent British Airways flight data recording wind vector and temperature observations (the Global Aircraft Data Set [GADS] archive) in three ways: (a) as an independent check of operational analyses; (b) as an analysis observing system experiment (OSE) as if the GADS observations were available in real time; and (c) as the corresponding forecast simulation experiment applicable to future operational forecasts. Using a 31 day sample (0000 UTC 20 December 2000 through 0000 UTC 20 January 2000) from Winter 2000, we conclude that over the data-dense continental U. S. analyzed jet streaks are too weak by -2% to -5%. Over nearby data-sparse regions of Canada, analyzed jet streaks are too weak by -5% to -9%. The second range provides a limit on the accuracy of current jet streak analyses over the portions of the ~85% of the earth's surface that are poorly covered by non-satellite observations. The -5% to -9% range is relevant for the pre-third generation satellite (AIRS, IASI, GIFTS) era.

When the additional GADS observations are treated as part of a hypothetical future observational data stream, they can produce modest (2-3%) changes in the analyzed wind speed even close to data-dense areas. Part of the problem is the difficulty in drawing to strong jets especially when the observations differ significantly from the first guess

forecasts.

Finally, for the limited but random sample chosen, the addition of the GADS observations produces a small but statistically significant improvement of ECMWF forecasts over short (24 hour; useful for aviation) and medium ranges (3-7 days). Such an effect occurs when the mean synoptic situation has strong jets in regions where GADS observations provide incremental information.

The GADS observations represent a hypothetical illustration of the kinds of additional aircraft observations in data-sparse regions that the WMO AMDAR panel is working to make operational. In particular, except for the Pacific where GADS observations are not available, the GADS observations hint at the asymptotic state possible from the use of commercial aircraft observations for the next decade. Further improvements in the depiction of strong jets and associated sharp thermal gradients await the third generation of satellite instruments. Once such data are included, current high-resolution (~7 km) GADS observations will again permit validation of atmospheric winds independent of any assimilation model. Efforts are underway to extend the GADS database to the Pacific.

Acknowledgments. We would like to thank: from British Airways: A. Aristocleous, D. Fleming, Q. Javed, M. Nebylowitsch, G. Selves, R. Smith, the staff of Flight Technical Dispatch, and especially Capt. J. Rankin who has supported the GADS experiment from its inception; from ECMWF: G. Kelly; from NASA: R. Atlas, K. Bergman, G. Brin, D. Dee, R. Gelaro, M. Helfand, Y. Kondratyeva, L.-P. Riishojgaard, R. Rood, M. Sienkiewicz, and Y. Sud; from SUNY Purchase: M. Oztunali; and from the United Kingdom Meteorological Office: R. Lunnon and G. Rickard. This research was supported in part by NASA Grants NAG52700 and NAG59370.

REFERENCES

Benjamin, S.G., B.E. Schwartz, and R.E. Cole, 1999: Accuracy of ACARS wind and temperature observations determined by collocation. *Wea. Forecasting*, **14**, 1032-1038.

Cheruy, F., J. Susskind, N. A. Scott, A. Chedin, and J. Joiner, 1993: GLA and LMD Approaches to the Processing of AIRS and IASI Observations in *High Spectral Resolution Infrared Remote Sensing for Earth's Weather and Climate Studies.* A. Chedin, M. T. Chahine, and N. A. Scott, ed. Springer-Verlag, Berlin, Heidelberg, 101-112.

Courtier, P., J. Derber, R. Errico, J.-F. Louis, and T. Vukicevic, 1993: Important literature on the use of adjoint, variational methods and the Kalman filter in meteorology. *Tellus*, **45A**, 342-357.

Cote, J., J.-G. Desmarais, S. Gravel, A. Methot, A. Patoine, M. Roch, and A. Staniford, 1998: The operational CMC/MRB Global Environmental Multiscale (GEM) Model. Part I and II. *Mon. Wea. Rev.*, **126**, 1373-1418.

Daley, R., 1991: *Atmospheric Data Analysis.* Cambridge University Press, 457pp.

Hoskins, B. J., and P. J. Valdes, 1990: On the existence of storm tracks. *J. Atmos. Sci.*, **47**, 1854-1864.

Kanamitsu, M., W. Ebisuzaki, J. Woolen, J. Potter, and M. Fiorino, 1999: An Overview of Reanalysis-2. *Proceedings of the Second WCRP International Conference on Reanalyses*, Wokefield Park nr. Reading, UK 23-27 August 1999.

McNally, A. P., J. C. Derber, W.-S. Wu and B. B. Katz, 2000: The use of TOVS level-1B radiances in the NCEP SSI analysis system. *Quart. J. Roy. Meteor. Soc.*, **126**, 689-724.

Parrish, D. F. and J. C. Derber, 1992: The National Meteorological Center's spectral statistical interpolation analysis system. *Mon. Wea. Rev.*, **120**, 1747 - 1763.

Pfaendtner, J., and S. C. Bloom, D. Lamich, M. Seablom, M. Sienkiewicz, J. G. Stobie, and A. M. da Silva, 1994: Technical Report Series on Global Modeling and Data Assimilation, Volume 4 - *Documentation of the Goddard Earth Observing System (GEOS) Data Assimilation System-Version 1*, NASA Technical Memorandum 104606 [available from National Technical Information Service Springfield, Virginia 22161].

Rickard, G. J., R. W. Lunnon, and J. Tenenbaum, 2001: The Met Office upper air winds: Prediction and verification in the

context of commercial aviation data. *Meteorol. Appl.*, **8**, 351-360.

Rukhovets, L., J. Tenenbaum, and M. Geller, 1998: The impact of additional aircraft data on the Goddard Earth Observing System analyses. *Mon. Wea. Rev.*, **126**, 2927-2941.

Saunders, F., 2000: The December 1999 European storms. NWP Gazette. [Available from The Met Office, London Road, Bracknell, Berkshire RG12 2SZ, United Kingdom.]

Tenenbaum, J., 1991: Jet stream winds: Comparisons of analyses with independent aircraft data over southwest Asia. *Wea. Forecasting*, **6**, 320-336.

-----, 1992: Operational impact of wind analysis errors on Southwest Asia aircraft routes. *ICAO Journal*, **47**, 12-13.

-----, 1996: Jet stream winds: Comparisons of aircraft observations with analyses. *Wea. Forecasting*, **11**, 188-197.

Uppala, S., J. K. Gibson, M. Fiorino, A. Hernandez, P Kållberg, X. Li, K. Onogi, and S. Saarinen, 1999: ECMWF second generation reanalysis - ERA40. *Proceedings of the Second WCRP International Conference on Reanalyses*, Wokefield Park nr. Reading, UK 23-27 August 1999.

WMO, 1996: *WMO Guide to Meteorological Instruments and Methods of Observation*. WMO No. 8. Geneva, Switzerland.

Figure Captions

Fig. 1. Example of a perpendicular jet stream crossing. ECMWF wind speed analysis at 250 hPa for (a) 1200 UTC 26 December 1999 and (b) 0000 UTC 27 December 1999.. Portions of the GADS aircraft trajectory are plotted as black dots with the observed location of the wind speed maxima of 88.5 m s^{-1} at 2109 UTC 26 December 1999 highlighted as a white dot. Contour interval, 5 m s^{-1}.

Fig. 2. Example of a parallel jet stream crossing. ECMWF wind speed analysis at 250 hPa for (a) 0000 UTC 23 December 1999 and (b) 1200 UTC 23 December 1999. Portions of the GADS aircraft trajectory are plotted with the observed location of the wind speed maxima of 98.3 m s^{-1} at 0824 UTC 23 December 1999 highlighted as in Fig. 1. Contour interval, 5 m s^{-1}.

Fig. 3. ECMWF aircraft data census for periods before and after the efforts of the AMDAR program. (a) 0000 UTC 17 March 2001, enlarged views of North America for (b) 0000 UTC 17 March 1999, (c) 0000 UTC 17 March 2001 [same as (a)]. Color key: red are manually transmitted AIREPs, green are ACARS, and blue are AMDAR reports.

Fig. 4. ECMWF quality control, analysis, and GADS observations for 1200 UTC 25 December 1999. (a) Aircraft observations between

200 and 300 hPa. Quantities plotted are aircraft observations minus first guess for accepted (green) and rejected (red) wind vectors, 250 hPa isotachs (contour interval, 10 m s^{-1}) and (thinned) locations of independent GADS aircraft observations from an off-peak hours Mexico City - London flight (black dots). (b) One-dimensional plot of the Mexico City - London GADS wind speed observations and ECMWF analyses at 217 hPa (37 000 ft). Plotted lines are GADS aircraft observations (red squares), ECMWF control analysis (green circles), and ECMWF analysis with GADS observations included (blue triangles).

Fig. 5. (a) ECMWF wind speeds at 250 hPa for 1200 UTC 11 January 1999 control analysis (contour interval, 5 m s^{-1}) and (b) corresponding ECMWF difference between analyses with and without GADS observations included (contour interval, 2 m s^{-1}). (c) DAO wind speeds at 250 hPa for 0000 UTC 22 December 1999 control analysis (contour interval, 5 m s^{-1}) and (d) corresponding DAO difference between analyses with and without GADS observations included (contour interval, 2 m s^{-1}).

Fig. 6. Winter period (see Table 1 for dates) average at 1200 UTC of the 300 hPa geopotential height and the 24-hour amplification factor for the most unstable Eady mode in the 700-850 hPa layer. (a) Winter 1999 period. (b) Winter 2000 period. (Contour intervals: geopotential, 100 m; dimensionless amplification factor, 0.1).

Fig. 7. One day data coverage of GADS observations. Only the GADS aircraft observations that do not depict real-time aircraft observations (AMDAR, ACARS and AIREP) are depicted.

Fig. 8. Root mean square error of the 500 hPa 24-hour ECMWF vector wind verified against its own analysis averaged over a) Europe b) North Atlantic c) North America and d) North Pacific.

Fig. 9. Time dependence of the 500 hPa geopotential height anomaly correlation verified against radiosonde observation for Winter 1999. a) Northern Hemisphere b) Southern Hemisphere.

Fig. 10. Time dependence of the 500 hPa geopotential height anomaly correlation verified against radiosonde observation for Winter 2000. a) Northern Hemisphere b) Southern Hemisphere.

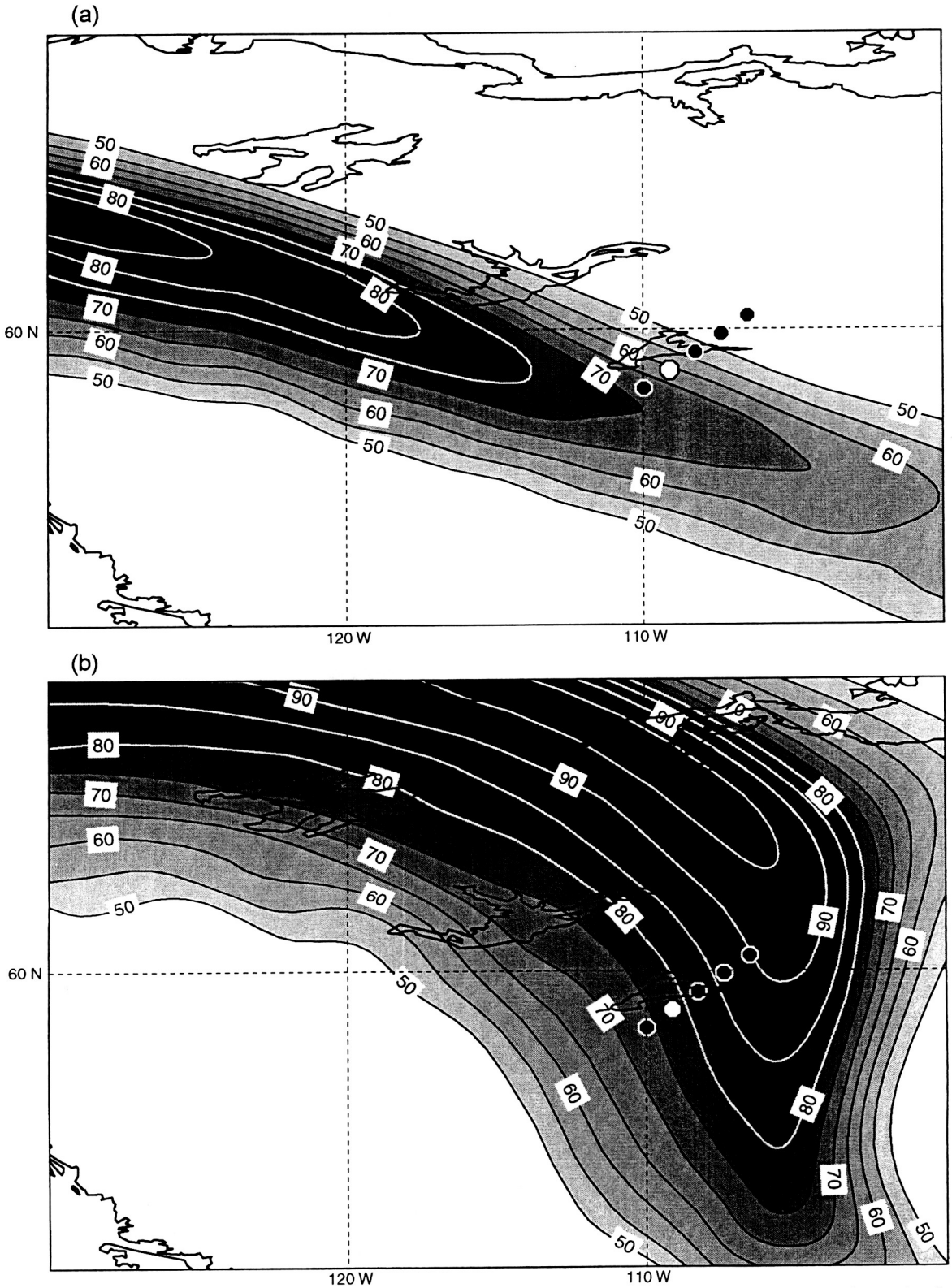

Fig. 1. Example of a perpendicular jet stream crossing. ECMWF wind speed analysis at 250 hPa for (a) 1200 UTC 26 December 1999 and (b) 0000 UTC 27 December 1999. Portions of the GADS aircraft trajectory are plotted as black dots with the observed location of the wind speed maxima of 88.5 m/s at 2109 UTC 26 December 1999 highlighted as a white dot. Contour interval, 5 m/s.

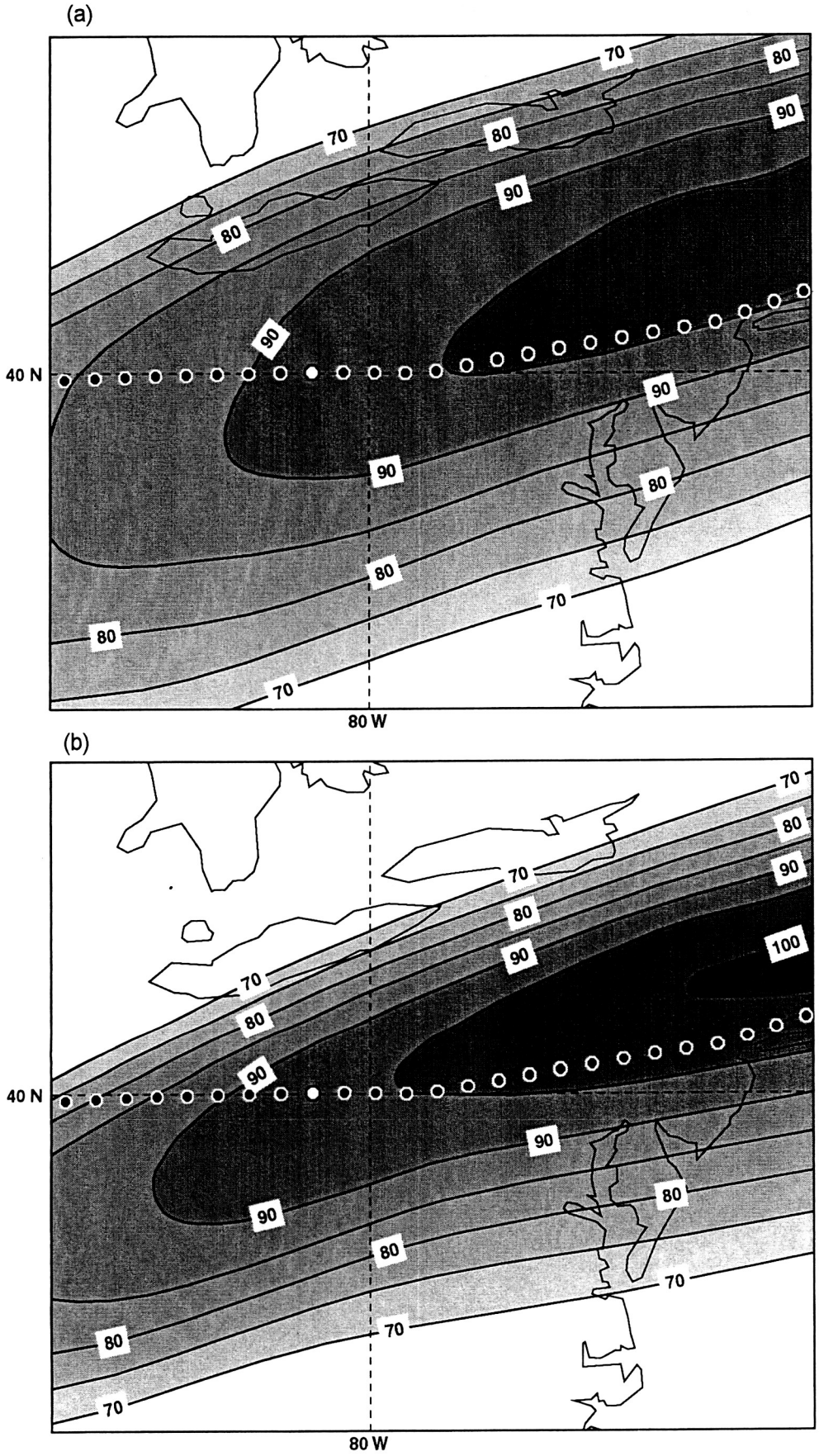

Fig. 2. Example of a parallel jet stream crossing. ECMWF wind speed analysis at 250 hPa for (a) 0000 UTC 23 December 1999 and (b) 1200 UTC 23 December 1999. Portions of the GADS aircraft trajectory are plotted with the observed location of the wind speed maxima of 98.3 m/s at 0824 UTC 23 December 1999 highlighted as in Fig. 1. Contour interval, 5 m/s.

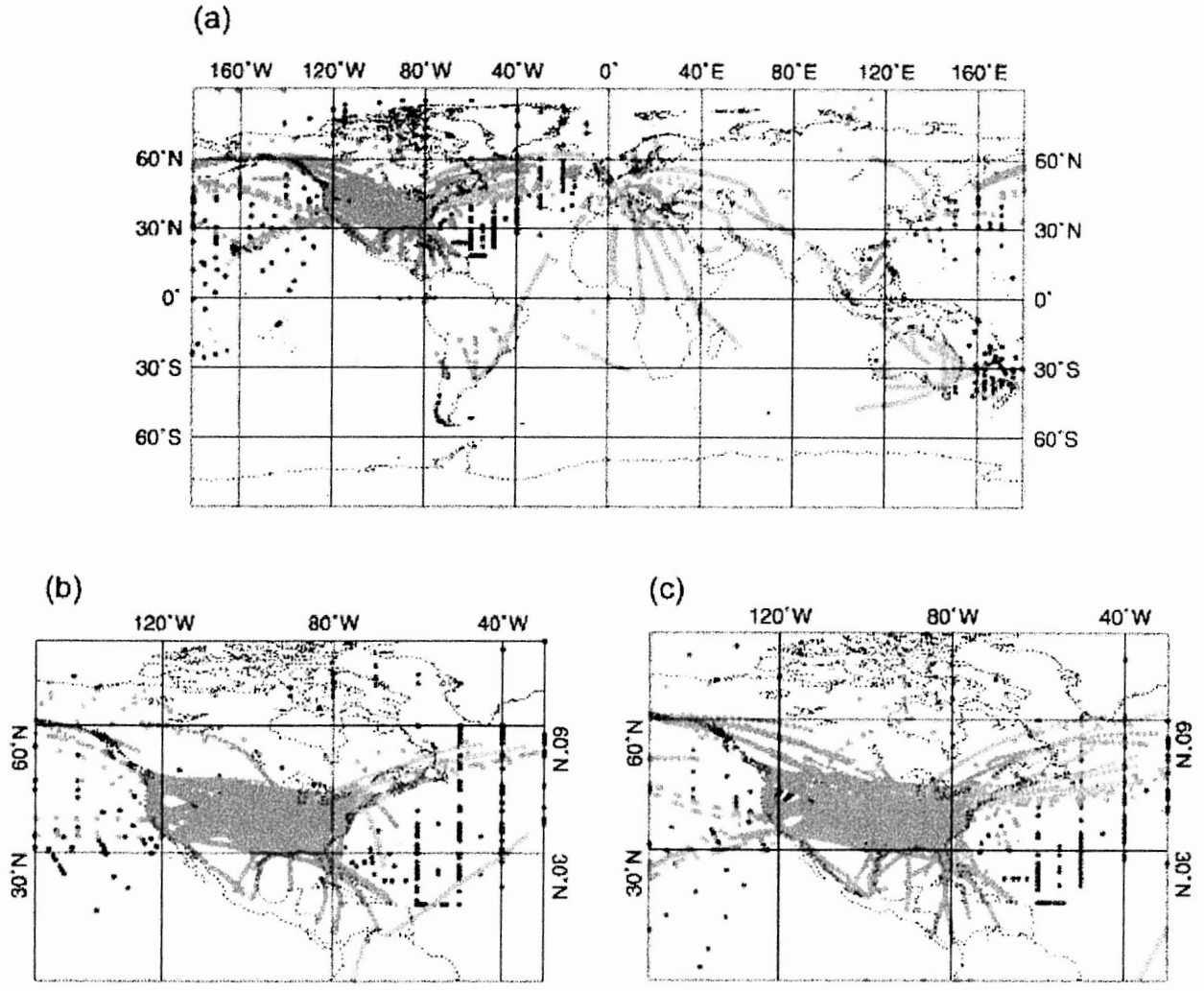

Fig. 3. ECMWF aircraft data census for periods before and after the efforts of the AMDAR program. (a) 0000 UTC 17 March 2001, enlarged views of North America for (b) 0000 UTC 17 March 1999, (c) 0000 UTC 17 March 2001 [same as (a)]. Color key: red are manually transmitted AIREPs, green are ACARS, and blue are AMDAR reports.

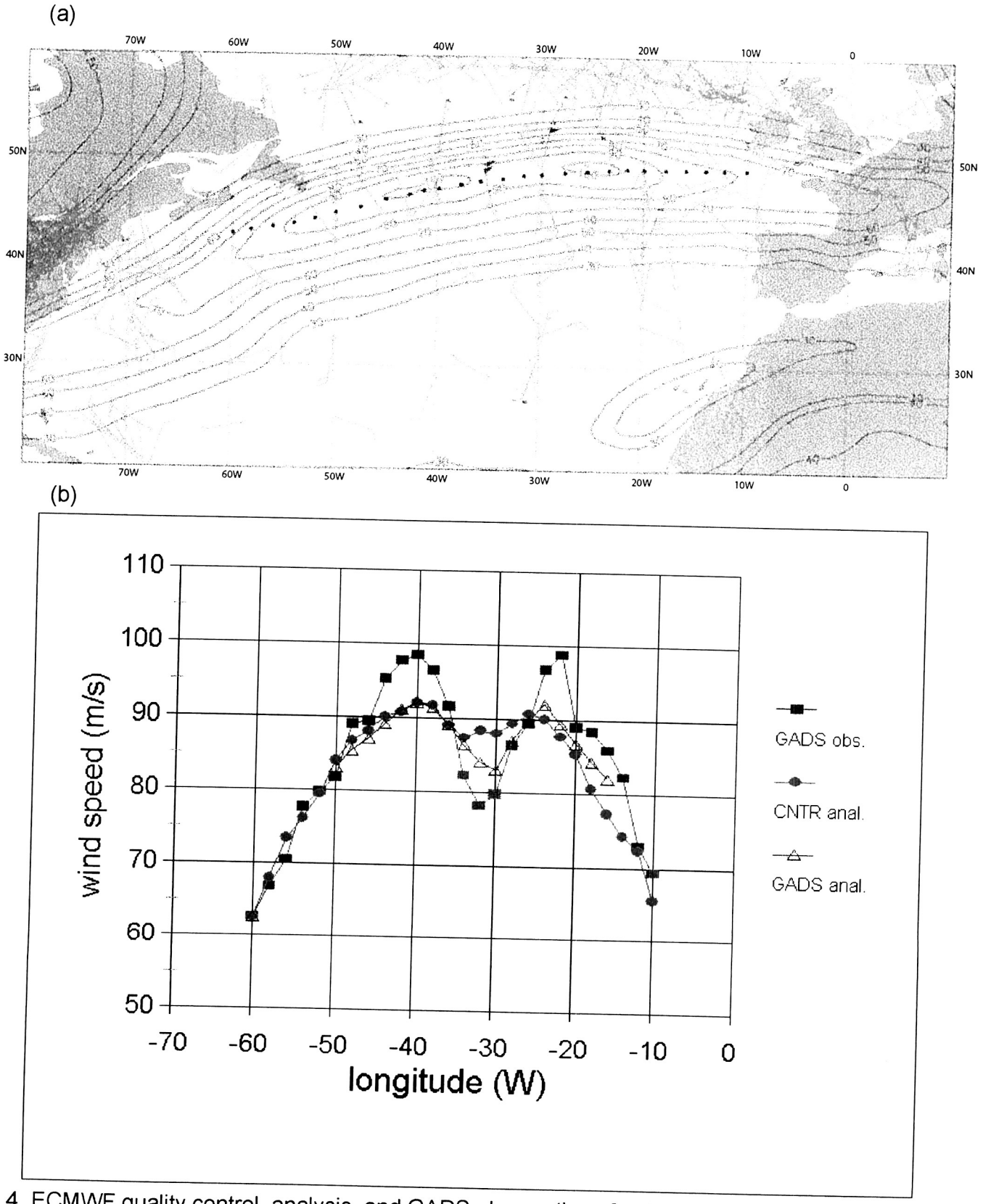

Fig. 4. ECMWF quality control, analysis, and GADS observations for 1200 UTC 25 December 1999. (a) Aircraft observations between 200 and 300 hPa. Quantities plotted are aircraft observations minus first guess for accepted (green) and rejected (red) wind vectors, 250 hPa isotachs (contour interval, 10 m s-1) and (thinned) locations of independent GADS aircraft observations from an off-peak hours Mexico City - London flight (black dots). (b) One-dimensional plot of the Mexico City - London GADS wind speed observations and ECMWF analyses at 217 hPa (37 000 ft). Plotted lines are GADS aircraft observations (red squares), ECMWF control analysis (green circles), and ECMWF analysis with GADS observations included (blue triangles).

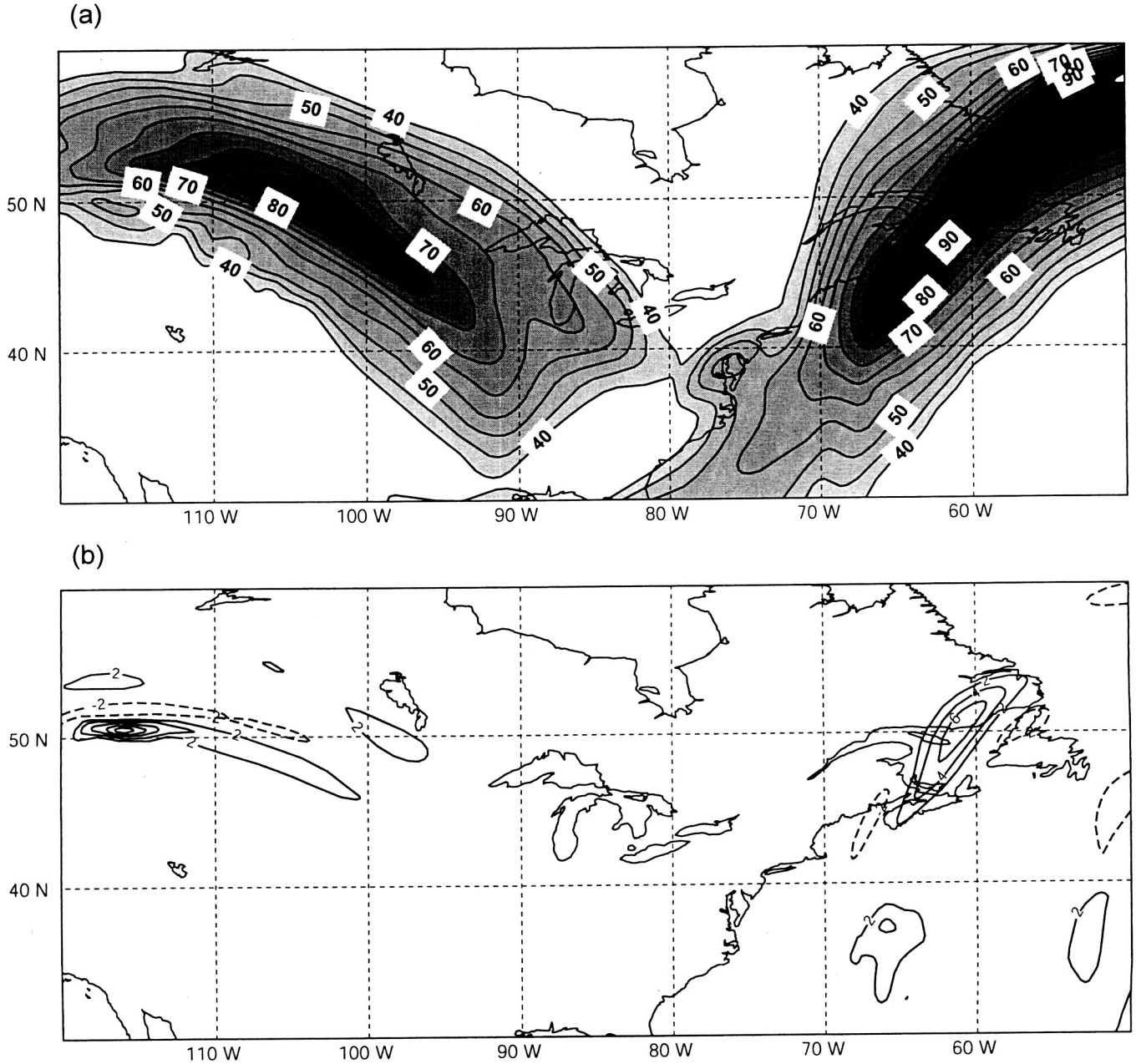
(a)
50 N
40 N
110 W
100 W
90 W
80 W
70 W
60 W
(b)
50 N
40 N
110 W
100 W
90 W
80 W
70 W
60 W

Fig. 5a,b

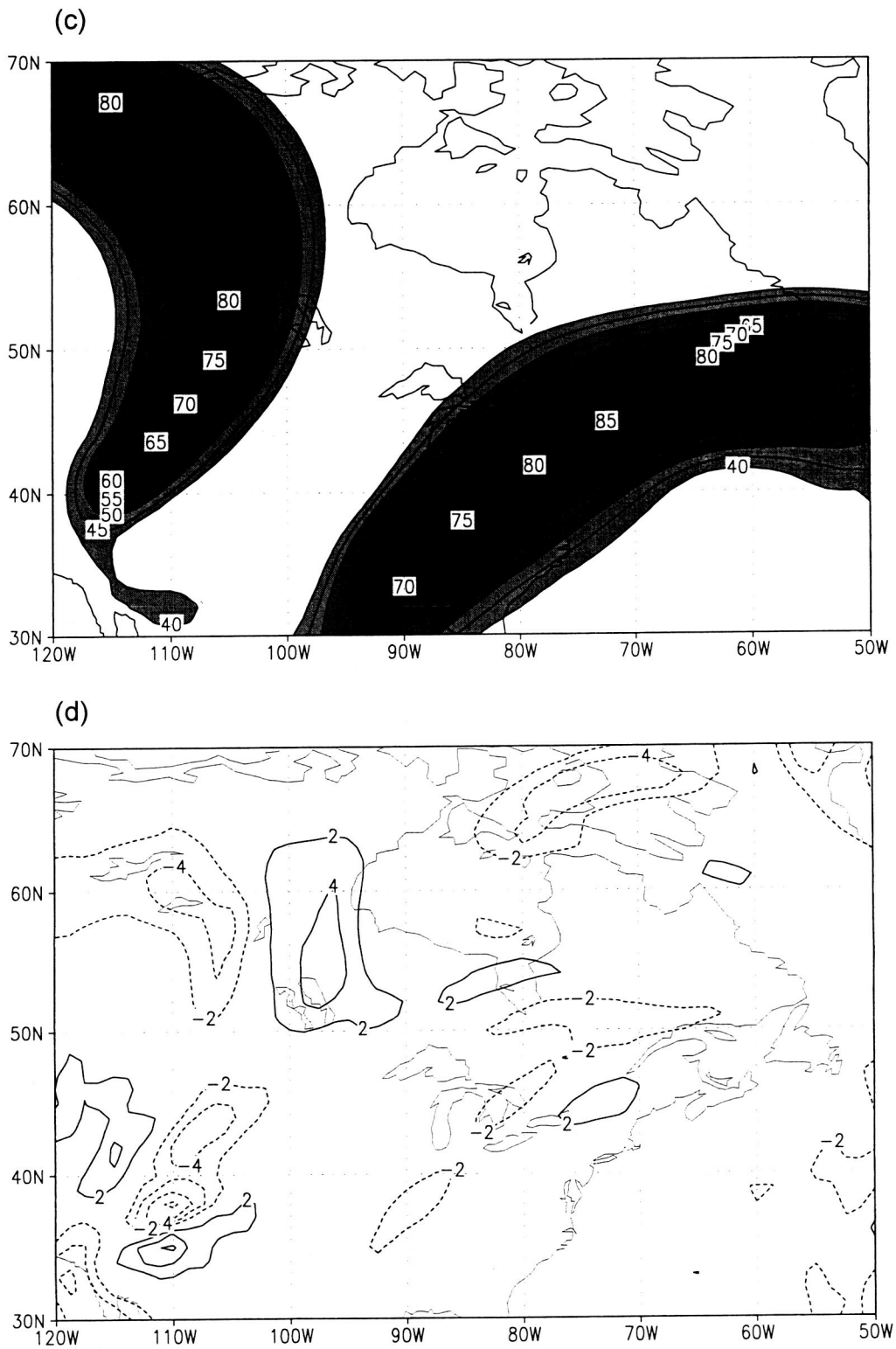

Fig. 5. (a) ECMWF wind speeds at 250 hPa for 1200 UTC 11 January 1999 control analysis (contour interval, 5 m/s) and (b) corresponding ECMWF difference between analyses with and without GADS observations included (contour interval, 2 m/s). (c) DAO wind speeds at 250 hPa for 0000 UTC 22 December 1999 control analysis (contour interval, 5 m/s) and (d) corresponding DAO difference between analyses with and without GADS observations included (contour interval, 2 m/s).

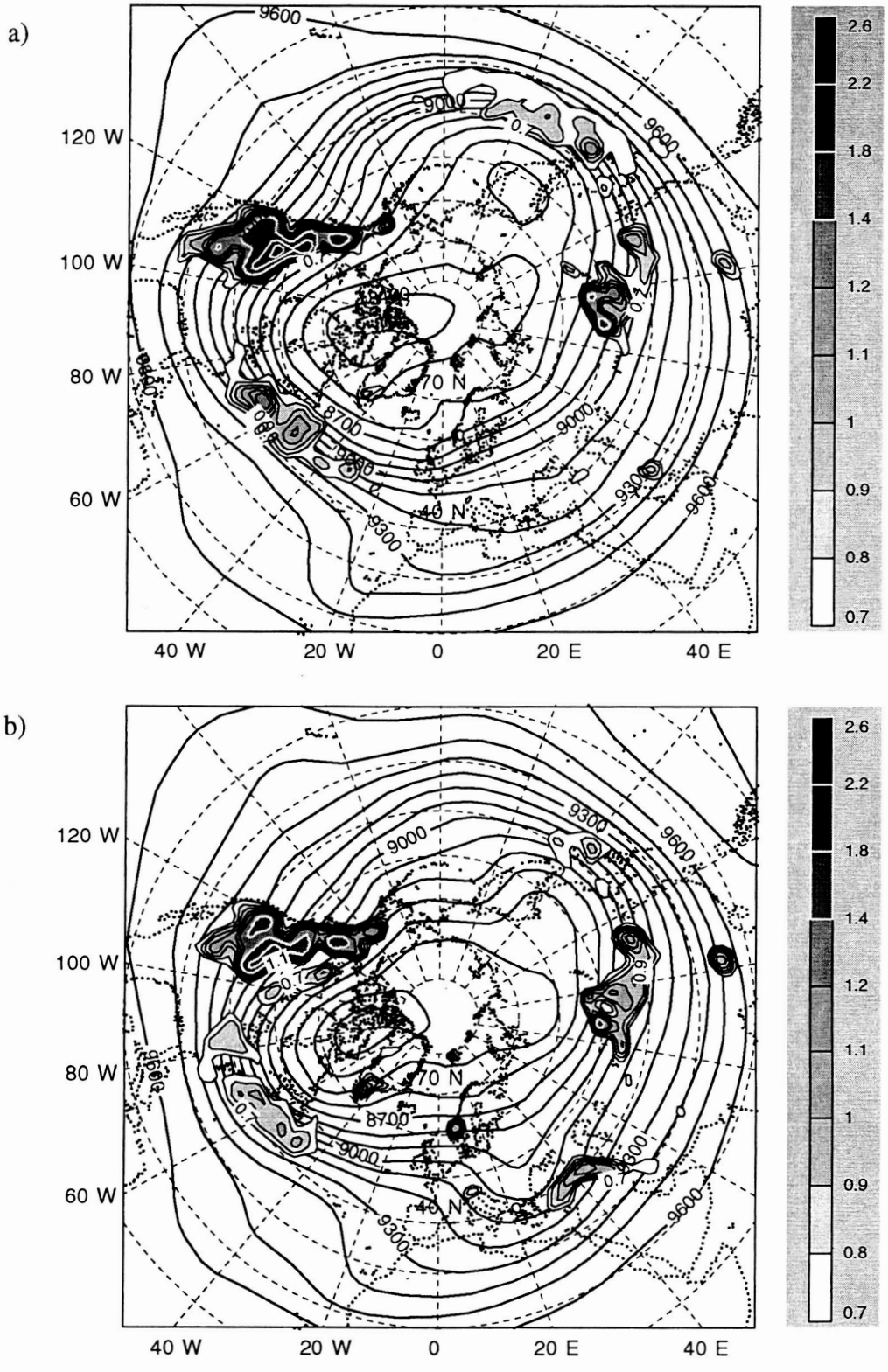

Fig. 6. Winter period (see Table 1 for dates) average at 1200 UTC of the 300 hPa geopotential height and the 24-hour amplification factor for the most unstable Eady mode in the 700-850 hPa layer. (a) Winter 1999 period. (b) Winter 2000 period. (Contour intervals: geopotential, 100 m; dimensionless amplification factor, 0.1).

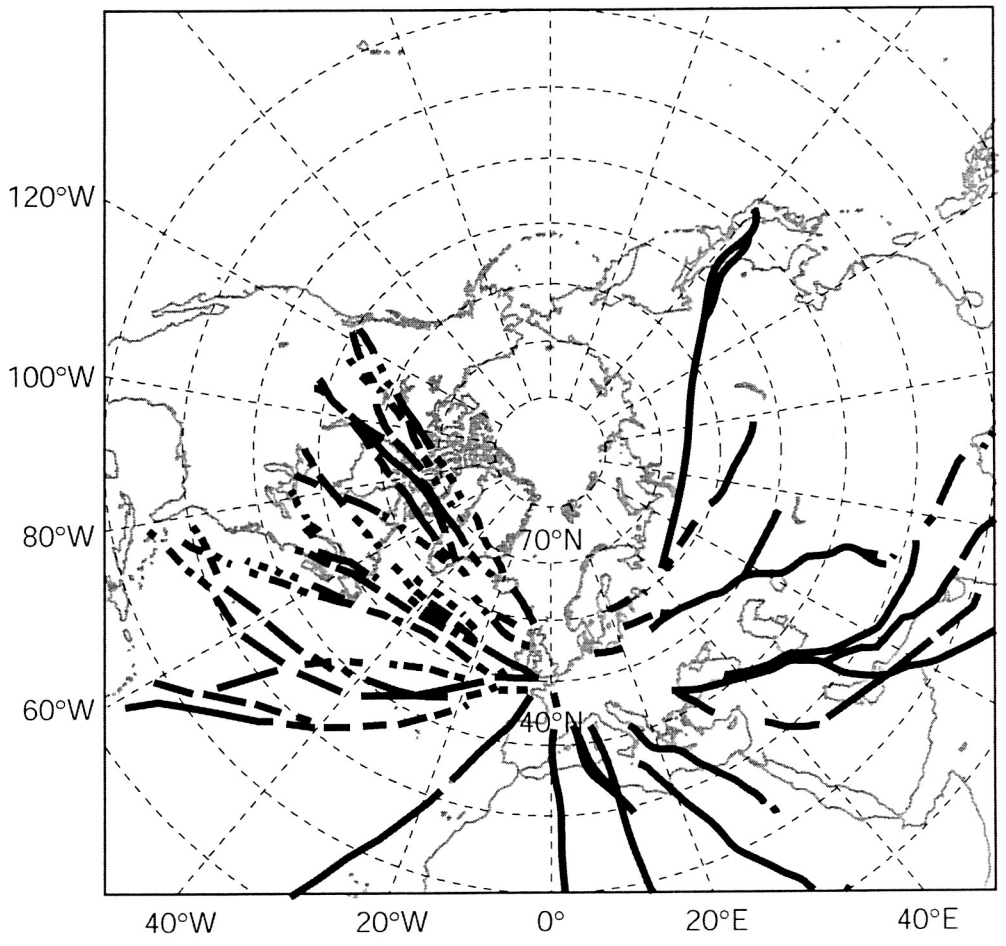

Fig. 7. One day data coverage of GADS observations. Only the GADS aircraft observations that do not depict real-time aircraft observations (AMDAR, ACARS and AIREP) are depicted.

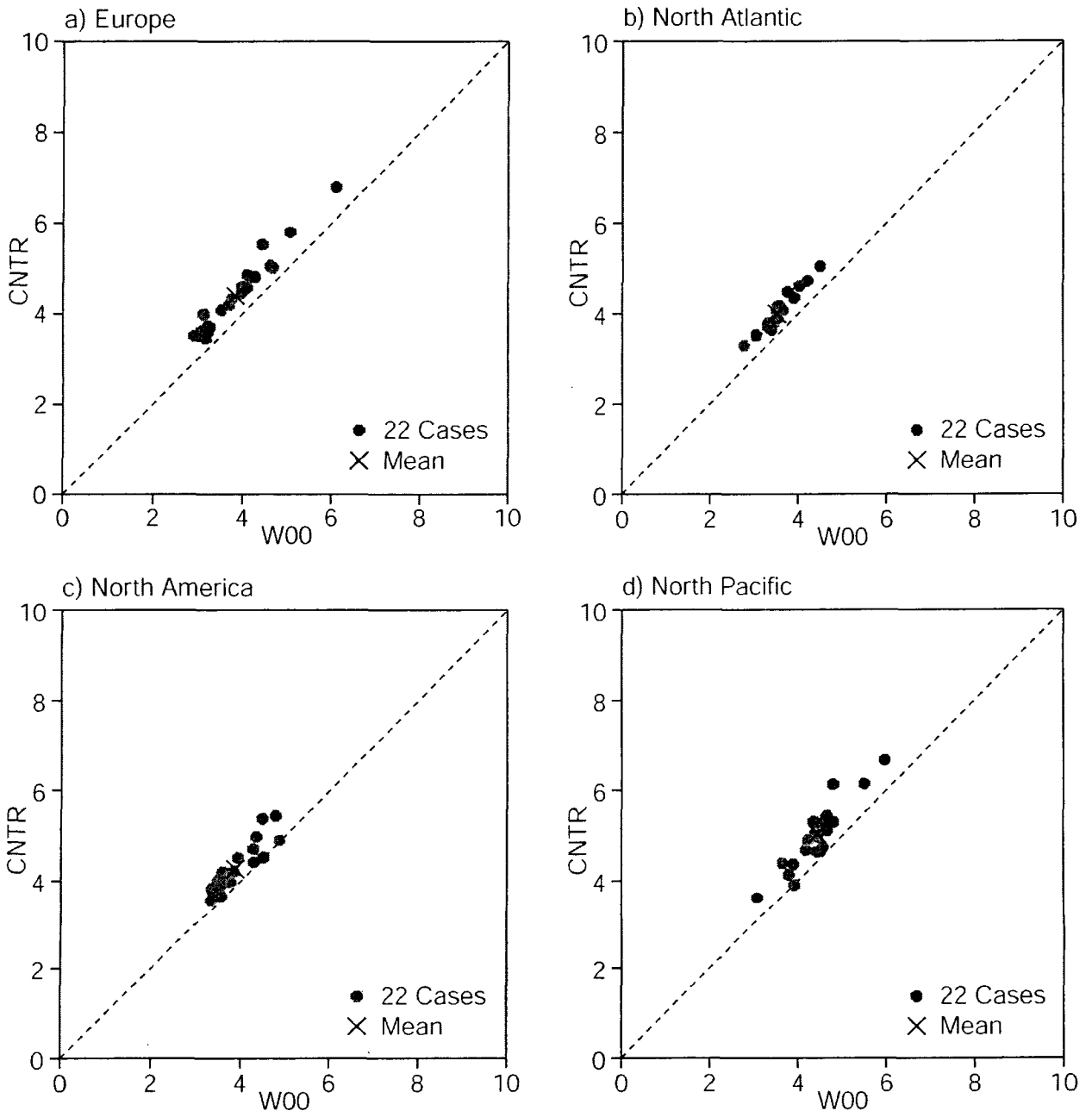

Fig. 8. Root mean square error of the 500 hPa 24-hour ECMWF vector wind verified against its own analysis averaged over a) Europe b) North Atlantic c) North America and d) North Pacific.

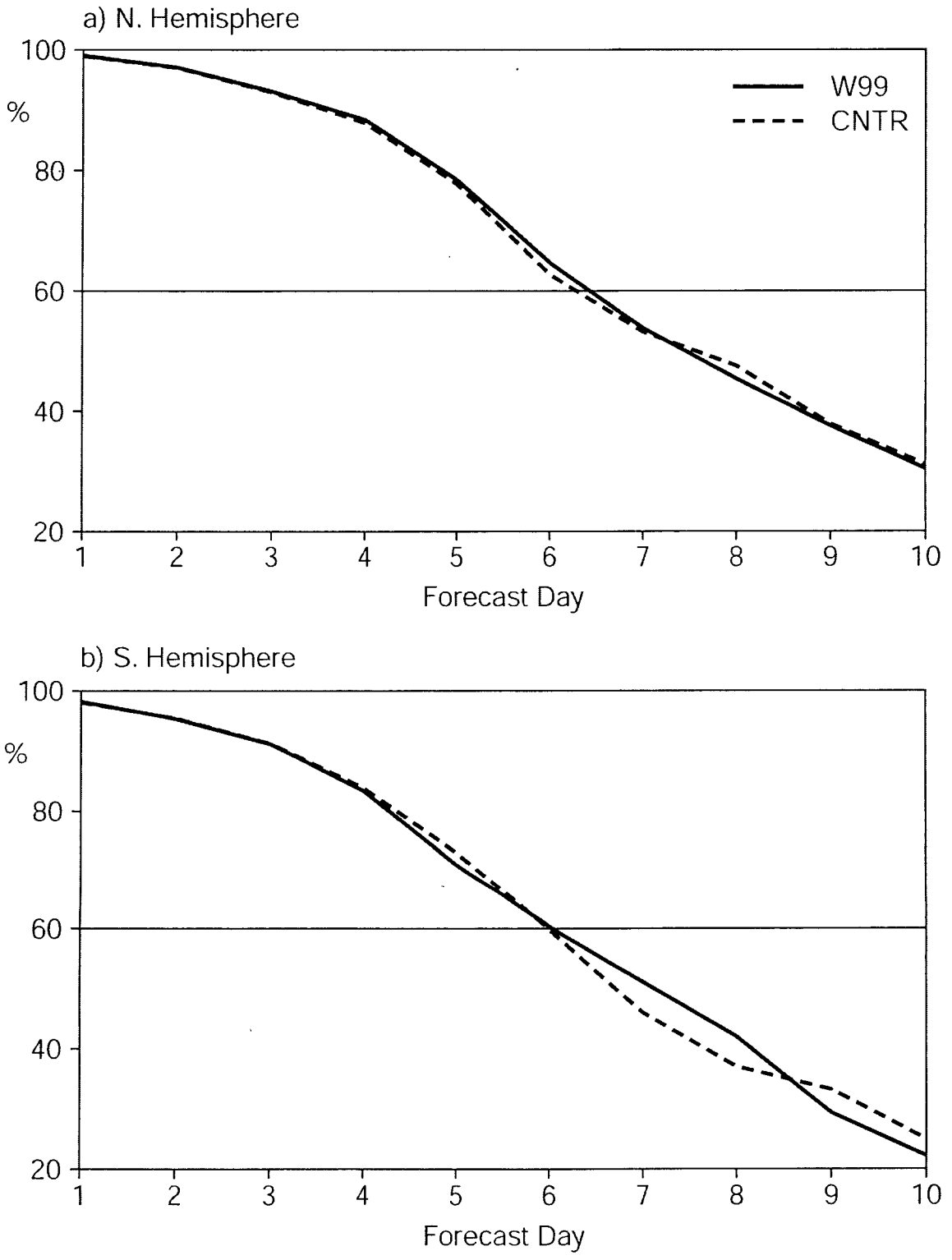

Fig. 9. Time dependence of the 500 hPa geopotential height anomaly correlation verified against radiosonde observation for Winter 1999. a) Northern Hemisphere b) Southern Hemisphere.

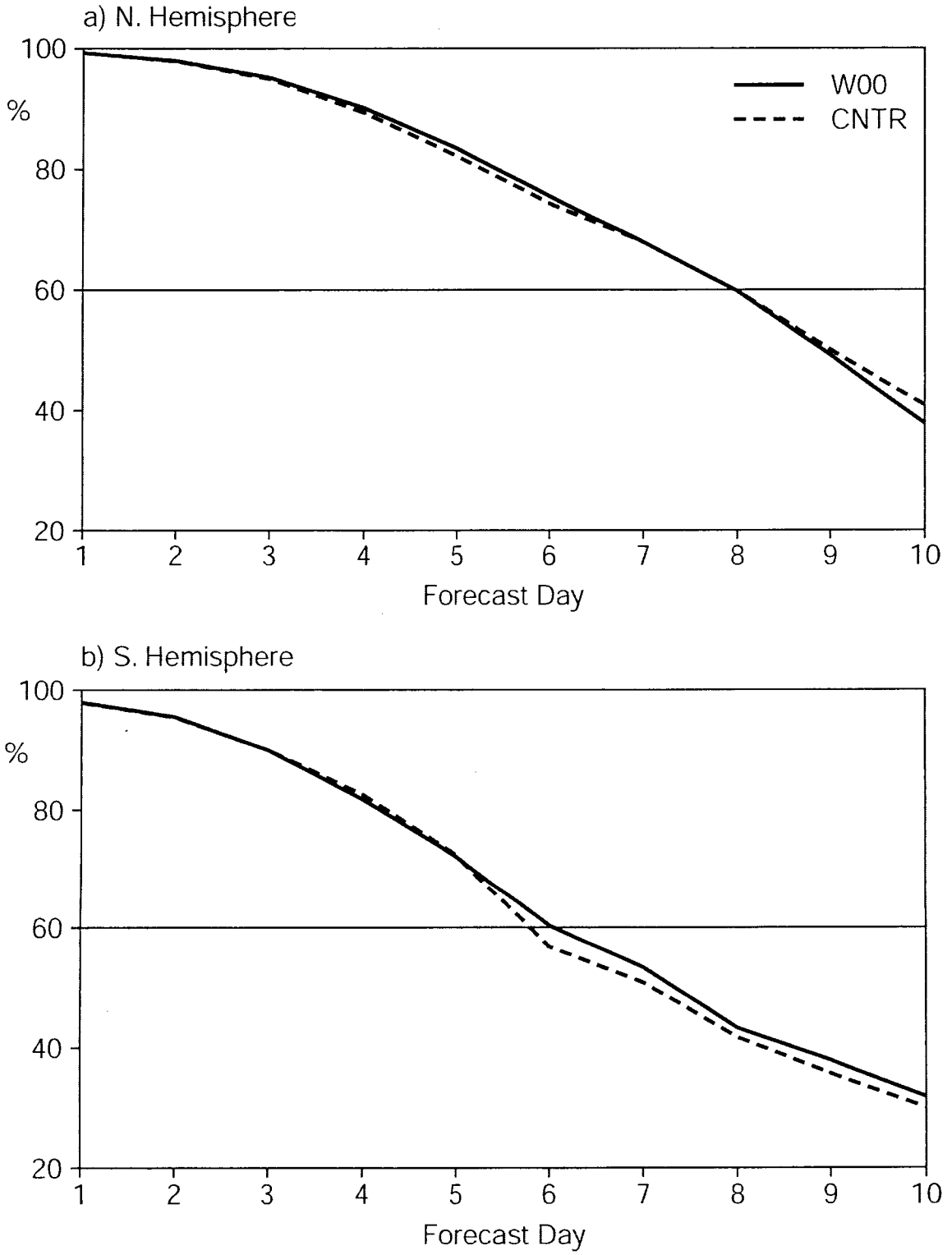

Fig. 10. Time dependence of the 500 hPa geopotential height anomaly correlation verified against radiosonde observation for Winter 2000. a) Northern Hemisphere b) Southern Hemisphere.